Published in final edited form as:
J Cell Physiol. 2008 November ; 217(2): 377–387. doi:10.1002/jcp.21507.

AGE-RELATED DIFFERENCES IN INSULIN-LIKE GROWTH FACTOR-1 RECEPTOR SIGNALING REGULATES AKT/FOXO3A AND ERK/FOS PATHWAYS IN VASCULAR SMOOTH MUSCLE CELLS

Muyao Li[1], **Jen-Fu Chiu**[2,3], **Jessica Gagne**[1,*], and **Naomi K. Fukagawa**[1,**]

[1]Department of Medicine University of Vermont College of Medicine, Burlington, VT 05405 USA

[2]Department of Biochemistry, University of Vermont College of Medicine, Burlington, VT 05405 USA

[3]Department of Anatomy, The Hong Kong University, Hong Kong, SAR, China

Abstract

Advanced age is a major risk factor for atherosclerosis, but how aging *per se* influences pathogenesis is not clear. Insulin-like growth factor-1 receptor (IGF-1R) promotes aortic vascular smooth muscle cell (VSMC) growth, migration, and extracellular matrix formation, but how IGF-1R signaling changes with age in VSMC is not known. We previously found age-related differences in the activation of Akt/FOXO3a and ERK1/2 pathways in VSMC, but the up-stream signaling remains unclear. Using explanted VSMC from Fischer 344/Brown Norway F1 hybrid rats shown to display age-related vascular pathology similar to humans, we compared IGF-1R expression in early passages of VSMC and found a constitutive activation of IGF-1R in VSMC from old compared to young rats, including IGF-1R expression and its tyrosine kinase activity. The link between IGF-1R activation and the Akt/FOXO3a and ERK pathways was confirmed through the induction of IGF-1R with IGF-1 in young cells and attenuation of IGF-1R with an inhibitor in old cells. The effects of three kinase inhibitors: AG1024, LY294002, and TCN, were compared in VSMC from old rats to differentiate IGF-1R from other upstream signaling that could also regulate the Akt/FOXO and ERK pathways. Genes for p27kip-1, catalase and MnSOD, which play important roles in the control of cell cycle arrest and stress resistance, were found to be FOXO3a-targets based on FOXO3a-siRNA treatment. Furthermore, IGF-1R signaling modulated these genes through activation of the Akt/FOXO3a pathway. Therefore, activation of IGF-1R signaling influences VSMC function in old rats and may contribute to the increased risk for atherosclerosis.

Keywords

Aging; IGF-1R; Akt/FOXO3a; ERK/Fos; VSMC; Glucose

Introduction

Age-associated changes in vascular structure and function are common to many species and occur in large arteries of rats, primates, and humans (Najjar et al, 2005). Aging is also a risk

**Address Correspondence to: Naomi K. Fukagawa, M.D., Ph.D., Department of Medicine, 89 Beaumont Avenue, Given Building, Room C207, Burlington, VT 05405; Tel: 802-656-4403; Fax: 802-656-2636; Naomi.Fukagawa@uvm.edu.
*Jessica Gagne's current address is the Millipore Corp., Andover, MA.

factor for the development of a variety of cardiovascular diseases, including atherosclerosis (Fried, 2000). One of the key elements in atherogenesis is the proliferation and migration of vascular smooth muscle cells (VSMC) (Dzau et al, 2002), which is accompanied by an increase in intimal-medial thickness and stiffness (Vazquez-Padron et al, 2004). VSMC have been found in lesions of the intima, and VSMC activity is likely to be critical in restenosis after angioplasty (Schwartz, 1997).

Various studies have shown that a number of membrane receptors, such as PDGFR, EGFR and VEGF-R/Fik-1, are involved in VSMC growth, migration, and extracellular matrix synthesis (Li and Xu, 2007), but few have been studied in the context of age-related differences. Recently, insulin-like growth factor-1 receptor (IGF-1R) was implicated to play a critical role in the control of lifespan (Holzenberger et al, 2003). When IGF-1R was mutated, organisms ranging from yeast to mice extended their life-span (Longo and Finch, 2003). In contrast, hyper-activation of the IGF-1R signaling pathway in $p44^{+/+}$ transgenic mice accelerated the progression of aging and shortened the maximum lifespan (Maier et al, 2004). These findings raise the possibility that IGF-1R may be partially responsible for the increased vulnerability to atherogenesis with advancing age.

Both IGF-1 and its receptor have been shown to be highly expressed in atherosclerotic lesions (Nichols et al, 1999; Scheidegger et al, 2000b). IGF-1R plays an important role in mediating Angiotensin II- and H_2O_2-induced mitogenesis of VSMC (Delafontaine et al, 1995;Azar et al, 2007). Targeted overexpression of IGF-1 in VSMC of transgenic mice enhances neointimal formation after intraarterial injury (Zhu et al, 2001) while dominant negative IGF-1R in VSMC inhibits neointimal formation (Lim et al, 2004). The activation IGF-1 signaling depends on binding of the ligand to its receptor, IGF-1R, which is abundant in the VSMC of intact arteries and in cultured VSMC (Arnqvist et al, 1995). IGF-1R is a tetrameric protein consisting of 2 extracellular α- and 2 intracellular β-chains. The β-chains include an intracellular tyrosine kinase domain that is thought to be essential for most of the receptor's biologic effects. IGF-1R signaling involves autophosphorylation and subsequent tyrosine phosphorylation of Shc and insulin receptor substrate (IRS). IRS serves as a docking protein and can activate multiple signaling pathways, including phosphatidyl inositol 3-kinase (PI3K), Akt, and mitogen-activated protein kinase (MAPK) (Delafontaine et al, 2004).

We previously reported that an age-related activation of Akt is responsible for the phosphorylation and inactivation of FOXO3a leading to down-regulation of MnSOD expression in explanted VSMC in early passages and isolated from young and old rats (Li et al, 2006b). We also found age-related differences in MAPK activities in VSMC from the young and old rats (Li et al, 2003). In earlier studies and in the present work, we employed the primary rat model of aging promoted by the National Institute on Aging (NIA) (Sprott and Ramirez, 1997), the Fischer 344/Brown Norway F1 hybrid (F344). Age-related progressive aortic vasculopathy and VSMC dysfunction in this rat model of aging have been reported (Blough et al, 2007;Miller et al, 2007), including the increase in aortic tissue content of Akt and MAPK with aging (Rice et al, 2005a;Rice et al, 2005b). Furthermore, several studies have reported that early passages of explanted VSMC retain their in vivo phenotype (Hariri et al, 1988; Spinetti et al, 2004). In the current study, we focused on the effect of the age of the animal on activation of IGF-1/IGF-1R signaling and its consequent effects on both the PI3K/Akt/FOXO3a and Raf/ERK/Fos pathways in explanted F344 VSMC. Furthermore, we determined how IGF-1/IGF-1R signaling influenced activation of target genes that regulate VSMC proliferation and detoxification enzymes. Understanding the regulation of specific pathways related to atherogenesis may lead to the development of specific therapies to reduce age-related vulnerability to disease.

Materials and Methods

Explanted aortic VSMC

Explanted VSMC were isolated from young mature (6-mo) and old (24-mo) male F344 rats purchased from Harlan-Sprague Dawley, Inc. (Indianapolis, IN), as described previously (Li et al, 2003). Rats were originally obtained from the NIH-NIA aging colonies and maintained in separate security barriers at Harlan Sprague Dawley according to the guidelines established in the Guide for the Care and Use of Laboratory Animals and under specific pathogen free conditions. VSMC at passages 3 or 4 were used in these experiments. Pairs of cell lines from one old and one young rat were grown and treated under identical conditions in each experiment as previously described (Li et al, 2006b). VSMC were grown in Dulbecco's Modified Eagle Media (DMEM), supplemented with 10% fetal bovine serum (FBS) and 1 unit/ml penicillin/streptomycin (PS) (Invitrogen, Carlsbad, CA) and containing normal glucose (5 mM) for 3 days or in same medium with high glucose (12.5 mM) for 3 days. To minimize changes in glucose concentrations over the 3-day period, the medium was changed every other day.

IGF-1 treatments

IGF-1 (Abcam Inc, Cambridge, MA) was diluted to a 1 μM stock solution in phosphate-buffered saline buffer. After subculturing, VSMC from young rats were grown on dishes or Nunc*lab-tek* II chamber-slides (Nalge Nunc International, Rochester, NY) overnight in complete DMEM medium containing 5 mM glucose. On the second day, medium was changed to reduced medium with 5 nM IGF-1 and the VSMC grown for 0.5, 1, 2, 4, 6, 8 or 24 h. A corresponding set of VSMC in reduced medium without IGF-1 was used as controls.

Kinase inhibitor treatments

AG-1024 was purchased from Calbiochem® (La Jolla, CA); LY294002 from Cell Signaling (Beverly, MA); and Triciribine (TCN) from Berry & Associates (Dexter, MI). Each of the inhibitors was prepared as a 20 mM stock by dissolving in DMSO. VSMC from old rats were grown in complete DMEM containing 5 mM glucose overnight after sub-culturing. On the second day, one set of dishes was pre-treated with 20 μM of each inhibitor in 5 mM glucose medium for 30 min, and then continuously grown in medium containing 5 mM or 12.5 mM glucose with 20 μM of each inhibitor, respectively, for 3 days. A corresponding set of cells was grown in the same medium without inhibitors, but with 1μl/ml DMSO as the vehicle control.

siRNA treatments

FOXO3a-siRNA SMARTpool (si-FOXO3a) was synthesized by Dharmacon, (Lafayette, CO) according to Rat LOC294515 (XM_215421) FOXO3a (predicted). VSMC were seeded into 100 mm dishes at 0.7×10^6/dish. After 24 h, the si-FOXO3a was diluted to a 2 μM working solution and delivered to cells at 100 nM final concentration for 48 hours through a lipid-mediated DharmaFECT Transfection Reagent (Dharmacon). A siCONTROL Cyclophilin B siRNA (Dharmacon) was also included as a transfection control.

Western blotting

Antibodies for IGF-1R β-chain were purchased from Biomol (Plymouth, PA); antibodies for FOXO3a, phospho-FOXO3a (Ser 253), Akt, phospho-Akt (Ser 473), ERK, phospho-ERK, phospho-JNK, P27kip-1, proliferating cell nuclear antigen (PCNA) from Cell Signaling (Danvers, MA); antibodies for catalase and β-actin from Abcam; antibody for MnSOD from OXIS (Foster City, CA); antibody for c-Fos from Santa Cruz (Santa Cruz, CA). Total, nuclear or cytoplasmic proteins were extracted from VSMC after each of the treatments.

Fifteen μg of each nuclear protein or 20 μg of total or cytoplasmic protein were electrophoresed on 10% SDS-PAGE gels and then electroblotted onto nitrocellulose membranes. The membranes were incubated with the appropriate primary antibody overnight with shaking at 4°C. After incubation with corresponding secondary antibodies, the protein bands were visualized using a SuperSignal™ West Pico Trial Kit (Pierce, Rockford, IL) and exposed to radiographic film. The blots were reprobed with a β-actin antibody to detect nuclear or total β-actin and used for normalization of the protein loading. The images and densities were captured with a GS-700 Imaging Densitometer (Bio-Rad, Richmond, CA) and analyzed with Quantity One Software Version 4.2 (Bio-Rad, Richmond, CA).

Tyrosine kinase phosphorylation assay

Five μg phosphotyrosine monoclonal antibody P-Tyr-100 (Cell Signaling) were added to 200 μg of cytoplasmic proteins, which were pre-diluted to 1 μg/μl with lysis buffer. The phosphorylated tyrosine proteins were immunoprecipitated (IP) overnight at 4°C. The immunocomplex was captured by a Protein G Agarose bead slurry (Upstate Chicago, IL) and then washed with lysis buffer. The agarose beads were then collected and boiled with 2× Laemmli sample buffer; then the supernatant was run on a SDS-PAGE for immunoblotting. The phosphorylated IGF-1R β-chain was identified by the IGF-1R β-chain antibody.

Electrophoretic mobility shift assay (EMSA)

Double stranded oligos (oligonucleotides) containing the MnSOD-DBE (Li et al, 2006b) were synthesized by Invitrogen as follows:

rSOD2P2a: 5'-ACAGTATGCTAACCTAAACAATTAAAGAGAA-3'

rSOD2P2b: 5'-TTCTCTTTTAATTGTTTAGGTTAGCATACTGT-3' (X5660: 1289)

An octamer-1 (OCT-1) consensus was used as an internal loading control:

OCT-1a: 5'-TGAGGGTATGCAAATTATTAAGAAGC-3'

OCT-1b: 5'-GCTTCTTAATAATTTGCATACCCTCA-3'.

The probes were labeled with [γ-^{32}P] ATP using T4 polynucleotide kinase and EMSA performed as described previously (Li et al, 2006a). A 100-residue of FOXO3a peptide (Abcam) containing the DNA binding domain and unmodified Ser 253 was included to confirmed the binding of FOXO3a to the MnSOD promoter.

Immunocytochemistry (ICC)

Cells grown on chamber-slides were fixed in 4% paraformaldehyde for 10 min, and then permeabilized with −20° C methanol for 5 min. After blocking in a PBS solution containing 1% BSA and 10% goat serum for 1 hour, 400 μl of 1 to 100–200 diluted mouse anti-IGF-1R β-chain (Biomol)/ rabbit anti-phospho-Akt (Cell Signaling), or mouse anti-phospho-Akt (Cell Signaling)/rabbit anti-FOXO3a (GenScrip, Piscataway, NJ) were applied onto each of the chamber slides, respectively, for overnight incubation at 4°C. Slides were then incubated with 1:400 diluted Alexa Fluor 488 anti-mouse and Alexa Fluor 568 anti-rabbit IgG (Molecular Probes Eugene, OR) at room temperature for 2 h, followed by 15 min with DAPI (Sigma-Aldrich). Finally the slides were examined using confocal laser scanning microscope LSM 510 (CSLM, Carl Zeiss Inc Thornwood, NY) and scanned for Alexa Fluor 488-staining (505–530 nm), Alexa Fluor 568 -staining (560–615 nm) and DAPI-staining (420–480 nm), respectively.

Real-time PCR

Total RNA was isolated from control and treated VSMC with UltraspecTM-II (Biotecx, Houston, TX). The first strand cDNA was synthesized in the reverse transcription reaction as follows: 1.5 purified RNA was added in 20 μl reverse transcription mixture containing 1μl MMLV reverse transcriptase (Invitrogen) and 1×MMLV RT buffer, 1μl random primers (Invitrogen), 0.25 mM dNTPs, 10 mM DTT and incubated at 42° C for 70 min followed by at 98° for 3 min. Expression of the IGF-1 and IGF-1R were quantified by Custom-designed TaqMan®Gene Expression Assay (Applied Biosystems, Foster City, CA):

RIGF-1-IGFF: 5'-ACAGACGGGCATTGTGGAT-3'

RIGF-1-IGFR: 5'-TCCAGCCTCCTCAGATCACA-3'

RIGF-1-IGFM: 5'-TCCGGAAGCAACACTC-3'

RIGF-1R-F: 5'-GGAGTGTCCATCAGGCTTCATC-3'

RIGF-1R-R: 5'-TTCATCGCCGCAGACCTT-3'

RIGF-1R-M: 5'-ACAGCACCCAGAGCAT-3'

Rat glyceraldehyde-3-phosphate dehydrogenase (GAPDH, Applied Biosystems, Assay ID: Rn01462661_g1) was used as a loading control. The cDNA samples were mixed with 24 μl master mixture (Applied Biosystems, Foster City, CA) in a 96-well TaqMan plate and amplified on an ABI Prism 7700 instrument (Applied Biosystems, Foster City, CA) by the Vermont Cancer Center DNA Analysis Facility at the University of Vermont.

RT-PCR

All RT-PCR primer sets were specifically designed crossing exons and synthesized by Invitrogen:

IGF-1F: 5'-TTCTACCTGGCACTCTGCTT-3' (M17335:276)

IGF-1R: 5'-CAAGCAGCAAAGGATCTTGC-3' (M17335:699)

IGF1R-F: 5'-TCCTCCGAGCTTAAGCAAGA-3' (NM_05287:3363)

IGF1R-R: 5'-CTCGCTGTAGTAGAAGGAGA-3' (NM_05287:3878)

FOXO3a-F: 5'-CGGACAAACGGCTCACTTT-3' (XM_215421:919)

FOXO3a-R: 5'-TCGGCTCTTGGTGTACTTG-3' (XM_215421:1190)

P27-F: 5'-AGGAGAGCTTGGATGTCAGC-3' (NM_031762: 733)

P27-R: 5'-CTGTTCTGTTGGCCCTTTTG-3' (NM_031762: 933)

CAT-F: 5'-TCTTCATCAGGGATGCCATG-3' (NM_012520: 541)

CAT-R: 5'-GTCTTCCTGCCTCTTCAACA-3' (NM_012520: 840)

MnSOD-2F: 5'-CAACTCAGGTTGCTCTTCA-3' (NM_017051:319)

MnSOD-R: 5'-CGACCTTGCTCCTTATTGA-3' (NM_017051:542)

After reverse transcription, PCR conditions (number of cycles and amount of cDNA, corresponding to template RNA) were defined to assure that the PCR reactions were run within linear range. 1–2 μl of cDNA was loaded into a total PCR mixture (20 μl) composed of 0.5 u Ampli Taq Gold, 1×PCR buffer with $MgCl_2$, 0.2 mM dNTPs, 22.5 nM of each forward or reverse primer. 1 μl QuantumRNA™ Universal 18S primers from Ambion (Austin, TX) was also included as an internal loading control in the PCR mixture, which was pre-mixed with the supplied Competimer at the ratio of 3:7. Rat ribosomal RNA L32 was

used instead of 18S when the size of the target band size was close to 18S. PCR was run under the following conditions: 94°C 14 min for 1 cycle; 94°C 1 min, 68°C 1min, 72°C 2 min for 14 cycles; 94°C 1 min, 55°C 1 min, and 72°C 2 min for 20 cycles; and a final extension at 72°C for 8 min and then visualized on 2% agarose gels. The standard curves were also set up with a series of diluted cDNA templates that assured a linear relationship between the cDNA concentration and the fluorescence of ethidium bromide.

Results

Age-related increase in IGF-1R activity in explanted VSMC

Knowing that the density of IGF-1R on the cell surface plays a critical role in triggering intracellular signaling cascades (Delafontaine et al, 1995), we determined whether there was an age-related difference in the expression of IGF-1R in VSMC from young and old rats. VSMC were grown in medium containing 5 mM glucose (normal or control) to mimic the *in vivo* situation and also grown in high glucose (12.5 mM) medium to introduce a mild, physiological stress to mimic the hyperglycemia often seen with advancing age. High glucose levels have been reported to induce moderate oxidative stress through the formation of advanced glycoxidation (AGEs) (Russell et al, 2002;Pennathur and Heinecke, 2007).

The density of IGF-1R β-chain was measured by Western blots. A sample of a Western blot is shown in the left panel of Figure 1A and a bar-graph summarizing the results from 4 pairs of young and old animals in the right panel. The β-chain density was 47 % higher in VSMC from old compared to young rats when grown in 5 mM glucose medium ($p = 0.03$). It remained ~ 38 % higher in VSMC from old rats cultured in 12.5 mM glucose medium ($p = 0.03$) than the levels in VSMC from young animals. However, exposure to 12.5 mM glucose medium for 3 days did not influence β-chain density (i.e. responsiveness) in VSMC from both young and old animals.

Since the IGF-1R β-chain includes an intracellular tyrosine kinase domain, which is essential for most of the receptor's biological effects, tyrosine kinase activities were compared in VSMC from young and old rats. Total phosphorylated tyrosine kinases were immunoprecipitated by the P-Tyr-100 antibody, and then the phosphorylation of IGF-1R was identified through immunoblotting with the anti-IGF-1R antibody. Figure 1B shows a representative blot on the left and a summary of results in 4 pairs of young and old animals on the right. By comparison, IGF-1R activity in VSMC from old rats was ~2.2 fold higher than the young when cells were grown in normal medium ($p = 0.01$). When cultured in 12.5 mM glucose medium, a 30% increase of IGF-1R activity was seen in young VSMC ($p < 0.01$) but not in old, thus diminishing the difference between young and old. In fact, IGR-1R activity appeared to be slightly lower in VSMC from old rats after exposure to high glucose but the difference between control and 12.5 mM glucose medium was not statistically significant ($p = 0.2$).

Having found an age-related constitutive increase in IGF-1R β-chain content and activity in VSMC, we sought to determine whether age affected gene expression of IGF-1R using both RT-PCR and Real-Time PCR. Figure 2A shows a representative RT-PCR result for IGF-1R (upper panel) and IGF-1 (lower panel). As shown in upper panel of Figure 2A, much brighter IGF-1R bands were observed in VSMC from old rats under both 5 mM and 12.5 mM glucose conditions; in contrast, their IGF-1 bands were relatively dim compared to young VSMC (lower panel of Figure 2A). Quantification of Real-Time PCR for IGF-1R from 4 pairs of young and old rats is summarized in Figure 2B. Results confirm the ~31% increase of IGF-1R mRNA in VSMC from old rats compared to young rats under basal conditions ($p < 0.05$). Similarly, the RT-PCR data for IGF-1 (Figure 2A) were confirmed by Real-Time PCR (data not shown). However, when VSMC were cultured in 12.5 mM

glucose medium, the expression of IGF-1R in cells from old rats was slightly reduced but remained ~20% higher than levels seen in VSMC from young rats (p <0.03). Together these findings demonstrate a constitutive increase of IGF-1R gene expression with older age but no evidence of an effect of IGF-1R on the response to high glucose medium.

IGF-1-induced activation of IGF-1R signaling influences both Akt and ERK pathways

We previously reported that IGF-1 treatment immediately triggered expression of IGF-1R β-chain in VSMC, followed by phosphorylation of Akt and inactivation of FOXO3a (Li et al, 2006b). In the current study, the ICC approach was used to establish a role for IGF-1R activation in the shuttling of phosphorylated Akt (P-Akt) and FOXO3a, which would explain the earlier findings of age-related differences in Akt /FOXO3a translocation. To do this, VSMC from young instead of old rats were used because of the constitutively higher level of IGF-1R in the old, which would make detection of changes more challenging. Hence VSMC from young rats were treated with IGF-1 (5 nM) to induce IGF-1R. Figure 3A shows the CLSM images from ICC experiments in two panels, and each includes three selected time sequences. In the upper panel of Figure 3A, VSMC were double stained for IGF-1R in green, P-Akt in red; and co-stained nuclei by DAPI in purple. IGF-1R and P-Akt were faintly stained in untreated young cells under control conditions (0 h); IGF-1R was greatly induced by IGF-1 treatment for 6 h and P-Akt became considerably abundant in the nuclei at 6 h; however, both were diminished after 24 h treatment (24 h). Meanwhile, in the lower panel of Figure 3A, VSMC were double stained for P-Akt in green and total FOXO3a in red. The P-Akt responses were the same as those stained in red in the upper panel. FOXO3a was mainly localized within the nuclei in the absence of IGF-1 (0 h), and remained in nuclei until 6 h of treatment with IGF-1. However, during the period from 0 to 6 h, some of the FOXO3a may have been phosphorylated, as suggested by our previous studies (Li et al, 2006b), but this could not be detected with the use of the FOXO3a antibody. After 24 h of treatment, the nuclei of the VSMC clearly became vacant, suggesting that translocation of FOXO3a into the cytoplasm occurred after 6 hours, later than the response of P-Akt. These ICC images confirmed that induction of IGF-1R was related to the shuttling of Akt/FOXO3a and support its role in upstream signaling for the Akt / FOXO3a pathway.

We also previously reported age-related differences in MAPK activity in VSMC, indicating there was ERK activation in VSMC from old rats, but not a Jun-N-terminal kinase (JNK) (Li et al, 2003). To determine whether IGF-1R is also related to the activation of the MAPK pathways, we examined the effect of IGF-1 treatment on the activation of phosphorylated JNK (P-JNK) and phosphorylated ERK (PERK) through Western blotting. As shown in the left panel of Figure 3B, IGF-1 treatment was associated with induction of P-ERK1/2 in the cytoplasm at 1 h; in contrast, P-JNK did not show a corresponding increase over the same time period. In the right panel, Western blots using total protein further show that induction of P-ERK appeared as early as treatment with IGF-1 for 0.5 h.

Effects of kinase inhibitors on the down-regulation of P-Akt, P-FOXO3a and relocation of FOXO3a

Having found constitutive activation of IGF-1R in VSMC from old rats which consequently contributed to the up-regulation of both the Akt/FOXO3a and ERK pathways, we reasoned that suppression of IGF-1R with an inhibitor should attenuate both of these effects in VSMC from old animals. We used 20 μM AG1024 (Tyrphostin), a specific IGF-1R tyrosine kinase inhibitor (Parrizas et al, 1997), to block the IGF-1R effect in VSMC from the old. However, the Akt/FOXO3a and ERK pathways could also be regulated by other growth factors or membrane receptors. Therefore, to distinguish between the roles of IGF-1R signaling with other signaling pathways, we compared the AG1024 effect with two additional kinase inhibitors: 1) LY294002, which inhibits PI3K and blocks all of the upstream signaling,

including IGF-1R and 2) TCN, which inhibits Akt and blocks all downstream pathways, including Akt/FOXO3a. Representative Western blots from total protein are shown in Figure 4A and their corresponding bar graphs in Figure 4B. More than one band for Akt or FOXO3a is not unexpected as different phosphorylation sites would lead to a shift in the molecular weight of the protein.

The upper panel of Figure 4A shows the changes in P-Akt and P-FOXO3a on a single blot. After treatment with 20μM of each inhibitor, P-Akt was down-regulated by 35% with AG1024 ($p = 0.01$), 50% with LY294002 ($p<0.01$) and 40% with TCN ($p < 0.01$) in VSMC grown under normal (5 mM glucose) conditions. Growth in medium containing 12.5 mM glucose induced an 80% increase of P-Akt compared to VSMC grown in 5 mM glucose medium (lane 5 vs.1, $p = 0.04$). LY294002 and TCN each reduced PAkt by 61% ($p < 0.01$ and $p < 0.05$, respectively), but AG1024 did not attenuate P-Akt to the same degree as LY294002 nor TCN under the stress of high glucose. This suggests that IGF-1R signaling contributed less to the activation of Akt under the metabolic stress of 12.5 mM glucose medium than the other signaling pathways.

All changes in P-FOXO3a induced by the three inhibitors paralleled the changes in P-Akt, except for the increase in P-FOXO3a, which did not reach significance when VSMC were grown in the 12.5 mM glucose medium (lane 5 vs.1, $p = 0.11$). The AG1024 had less of an effect on P-FOXO3a than the other two inhibitors. In contrast, LY294002 had a maximal effect on P-FOXO3a, which was down-regulated by 46% ($p = 0.002$). To determine whether FOXO3a was relocated into the nucleus by repression of PFOXO3a formation, nuclear FOXO3a levels were examined. The results showed that nuclear FOXO3a levels were increased significantly (by 70%, $p = 0.02$) with AG1024 and 93% with TCN treatment ($p < 0.03$), but less with LY294002 when VSMC were grown in 5 mM glucose medium. These effects were not influenced by growth in the high glucose medium. The data suggest that the decrease in P-FOXO3a did not always parallel the increase in nuclear FOXO3a levels and that other pathways responsible for FOXO3a re-localization from the cytoplasm into the nucleus may be involved. In summary, IGF-1R activity influenced the P-Akt/FOXO3a pathway under basal conditions, but when VSMC were stressed by high glucose medium, alternative pathways become dominant.

Effects of kinase inhibitors on the down-regulation of P-ERK, c-FOS and PCNA

To determine whether the above inhibitors influenced the ERK pathway in the same manner as the P-Akt/FOXO3a pathway, the effects on P-ERK1/2 and downstream c-Fos, an AP-1 component, were examined. The representative Western blots are shown in Figure 5A and their corresponding bar graphs in Figure 5B. After treatment with 20μM of each inhibitor, the most inhibition of P-ERK1/2 was seen with AG1024 and LY294002 treatments ($p < 0.02$). Meanwhile, nuclear c-Fos was also significantly reduced by LY294002 treatment ($p < 0.03$). The effect of the Akt inhibitor TCN on ERK1/2 and c-Fos was minimal. These results suggest that the LY294002, which is primarily known for its blocking of the PI3K/Akt pathway, also inhibited the ERK/FOS pathway. These data are in agreement with those of other investigators (Nosaka et al, 2001; Menu et al, 2004) showing that PI3K is upstream of both the Akt/FOXO and ERK/Fos pathways.

Both the Akt/FOXO and ERK/Fos pathways are known for their mitogenic effects. Therefore, to confirm that the inactivation of these pathways would suppress VSMC proliferation, proliferating cell nuclear antigen (PCNA) was measured as a marker. The lower panel of Figure 5A shows the changes of PCNA expression when cells were exposed to the kinase inhibitors. Maximal inhibition of mitogenesis in the 5 mM glucose medium was observed after LY294002 treatment (67%, $p = 0.01$), followed by TCN (31%, $p < 0.03$). However, the 26% inhibition by AG1024 failed to achieve significance ($p = 0.057$). As

noted earlier with IGF-1 treatment (Figure 3B), IGF-1R signaling was not found to activate P-JNK. To confirm this result, we further compared AG1024 effects on P-JNK with the effects of LY294002. Figure 5C shows that AG1024 had less of an effect on P-JNK, whereas LY294002 greatly reduced P-JNK levels when VSMC were grown in both 5 mM and 12.5 mM glucose media.

Effects of FOXO3a-SiRNA on down-regulation of p27, MnSOD and catalase expression

FOXO3a is the primary forkhead transcription factor expressed in VSMC (Lee et al, 2007). FOXO transcription factors play important roles in cell function, including ROS detoxification, DNA repair, cell cycle arrest and cell death (Carter and Brunet, 2007). In addition to transcriptional regulation of MnSOD by FOXO3a, which was previously revealed by Kops et al (Kops et al, 2002) in humans, and by us in the rat respectively, we have also reported reduced MnSOD level in old animals (Li et al, 2006b). In the current study, we examined effects of FOXO3a on the regulation of two other putative-target genes, a CDK inhibitor, p27kip-1 (p27) (Dijkers et al, 2000), which is responsible for G1 arrest, and catalase (Nemoto and Finkel, 2002). A pool of FOXO3a siRNA was used to block FOXO3a mRNA. The changes of gene expression were compared using semi-quantitative RT-PCR. As shown in Figure 6A from left to right, when the fluorescence of FOXO3a declined by 70% in FOXO3A-SiRNA treated cells relative to their scrambled controls, the fluorescence of p27, catalase and MnSOD were correspondingly reduced by 57%, 63% and 69%, respectively. Meanwhile, in Figure 6B, the expected reductions in protein levels were also observed through Western blots. These results demonstrate that FOXO3a is involved in transcriptional regulation of these three genes in rat VSMC under the present conditions.

Inhibition of IGF-1R signaling on restoration of p27, MnSOD and catalase expression

Having shown that FOXO3a-SiRNA blocked p27, catalase and MnSOD gene expression and that inactivation of IGF-1/Akt signaling by inhibitors could relocate FOXO3a in the nuclei; the next step was to determine whether these inhibitors could restore expression of FOXO3a target genes using Western blot analysis. A representative Western blot of each is shown in Figure 7A and its corresponding bar graphs in Figure 7B. VSMC did show a 30% increase of MnSOD with AG1024 ($p = 0.02$) and little with TCN in 5 mM glucose medium. Surprisingly, no MnSOD expression was restored when VSMC were treated with LY294002, which had a significant effect on suppression of mitogenesis. No clear changes were observed with the inhibiters when VSMC were cultured in 12.5 mM glucose medium. The result from the LY294002 treatment was confirmed by RT-PCR and EMSA as shown in Figure 7C. The MnSOD mRNA was increased over two-fold by AG1024 and TCN, but this was not seen with LY294002. The EMSA result indicates that the DNA binding detected by the MnSOD-DBE probe was enhanced with AG1024 but much less with LY294002. The specificity of MnSOD-DBE probe was determined with a 100-residue of FOXO3a peptide, which ran faster than the FOXO3a protein, but the result did demonstrate binding of the MnSOD-DBE probe to FOXO3a. Meanwhile, expression of catalase was significantly increased in VSMC grown in 5 mM glucose medium with each inhibitors, by 38% ($p = 0.01$), 34% ($p = 0.03$) and 56% ($p < 0.05$), respectively.

Western blots did not show any statistically significant differences in p27 protein levels between control and those treated with inhibitors in both kinds of media. To verify whether the inhibitors influenced p27 gene expression, quantitative RT-PCR was used. Figure 7D shows a representative RT-PCR that indicates an up to 2-fold increase of p27 mRNA with AG1024 and over 3-fold increases of p27 with LY294002 and TCN in 5 mM glucose medium. P27 was reported to contain an Akt consensus phosphorylation site in its nuclear localization motif. When phosphorylated by Akt, p27 impairs its nuclear import and accumulates in cytoplasm (Liang et al, 2002). When Akt kinase activity was reduced by the

inhibitors, this led to up-regulation of nuclear p27 levels (Shin et al, 2002). Hence the nuclear p27 level was examined. In contrast to total protein, the nuclear p27 protein did increase with the use of the inhibitors (Figure 7D).

Discussion

Dissecting the effects of local IGF-1 levels in VSMC is impractical because their complex distribution modulated by several high affinity binding proteins (Scheidegger et al, 2000a), and IGF-1R signaling could also be activated by IGF-II (Werner and Maor, 2006) and insulin ligands (Johansson and Arnqvist, 2006). Therefore, it is the IGF-1R, not IGF-1 *per se*, that plays a central role in "IGF-1 signaling". In this study, we have demonstrated constitutive activation of IGF-1R in explanted VSMC from old rats compared to young counterparts. The activation was substantiated by an increase in IGF-1R gene expression, surface density and tyrosine kinase activity. Together with our previous reports, we conclude that the activation of IGF-1R signaling in explanted VSMC triggers both PI3K/Akt and PI3K/ERK pathways, thereby contributing to down-regulation of stress-resistance and up-regulation of cell proliferation.

Although IGF-1R is reported to play a critical role in the control of lifespan, how expression of IGF-1R changes throughout the life is still unclear. Reports in the literature differ with the tissues and cell-types examined. Maier et al have reported that IGF-1R levels were found to be elevated in tissues of older p44 homozygous mice that continue to proliferate throughout life (testis and spleen), but not in tissues containing primarily postmitotic cells (Maier et al, 2004). This suggests that changes of IGF-1R expression with aging are tissue and cell type specific and especially dependent on their mitotic status. Aortic VSMC used in the present work are among the cells with the potential for proliferation. Recently, Miller et al reported a progressive increase in intimal and medial thickness as well as smooth muscle cell-containing intimal protrusions in old F344 rat aorta compared to the young. This structural vascular pathology was associated with a progressive increase in global differential gene expression based on microarray-analysis of RNA isolated from aortic tissue. The genes with altered expression between 3 and 28 month of age included a 2.8-fold increase in IGF-1R mRNA (Miller et al, 2007). This observation from in vivo analysis greatly supports our findings in explanted VSMC during early passages and is consistent with our premise that early passages of explanted VSMC retain their *in vivo* age-related characteristics. The present *in vitro* studies complement the *in vivo* descriptive studies by demonstrating the downstream effects of IGF-1R signaling.

The comparisons have been made in this study with different inhibitors that allow us to differentiate the function of IGF-1R from other signaling pathways. The age-related activation of IGF-1R has several interesting implications. The first is that IGF-1R activation is more constitutive than inducible. The age-related differences, either on IGF-1R expression or on its activity, were observed under basal condition (5 mM glucose medium) but did not show an increase when stressed by exposure to 12.5 mM glucose (Figure 1, 2). Furthermore, the effect of LY294002 on inhibition of P-Akt or P-FOXO3a was similar to AG1024 (Figure 4) in 5 mM glucose medium, indicating that the inhibitory effect of LY294002 is dependent on blocking IGF-1R signaling under these conditions. However, when challenged by 12.5 mM glucose medium, effects of LY294002 differed from the effects of AG1024, suggesting inhibition of multiple signaling pathways rather than IGF-1R alone.

Secondly, IGF-1R is more likely to down-regulate MnSOD than up-regulate VSMC proliferation. VSMC showed an increase of MnSOD when treated with AG1024, but not with LY294002. This is not surprising in that IGF-1R signaling seems particularly tied to the down-regulation of MnSOD since an IGF-1R mutation is closely related to the extension of

lifespan while the target gene mediating FOXO's ability to extend longevity is MnSOD (Honda and Honda, 1999). It is possible that FOXO's response to IGF-1R signaling differs from responses to other growth factors, like other investigators have hypothesized (Greer and Brunet, 2005). On the other hand, AG1024 showed minimal anti-proliferative effects compared to LY294002 (Figure 5, PCNA). Inhibition of PI3K with LY294002 involved blocking all upstream growth signals that switched cells from proliferation to growth arrest and apoptosis. Cell death is the opposite from stress resistance, which implies survival. Therefore, inhibiting PI3K may cause FOXO to induce those target genes related to cell death rather than the target genes related to resistance to oxidative stress (Greer and Brunet, 2005). This may be one reason why IGF-1R has a relatively mild effect on proliferation but has more of an effect on the down-regulation of MnSOD, and consequently, more of a relationship to the reduction in lifespan.

Thirdly, IGF-1R is more likely involved in the shuttling of FOXO3a out of nucleus than shuttling it into the nucleus. As shown in Figure 4, LY294002 more successfully inhibited phosphorylation of Akt than AG1024, which blocked the export of FOXO3a into the cytosol. However, LY294002 failed to keep FOXO3a in the nucleus as efficiently as AG1024. This phenomenon suggested that in addition to shuttling of the FOXO from the nucleus to the cytosol, cells must have another mechanism to reverse the shuttle. Cytoplasmic JNK was recently reported to have this function (Wang et al, 2005) and JNK/FOXO signaling appears to coordinate metabolism and stress defenses (Erol, 2007). As we have already determined that the age-related activation of IGF-1R is more related to activation of Akt or ERK and less to activation of JNK, it seems to follow that IGF-1R more likely affects shuttling FOXO out of nucleus than shuttling into the nucleus. In contrast, most other growth factors or membrane receptors are known to activate Akt as well as the JNK pathway, such as TGF-β (Utsugi et al, 2003) or EGF (Manfroid et al, 2005), and in that way better maintain the balance between the export of FOXO by Akt with the import FOXO by JNK. The PI3K inhibitor, LY294002, inhibits these growth factors leading to simultaneous blocking of Akt and JNK activity, while AG1024 only inhibits Akt. This may explain why LY294002 failed to sustain FOXO3a in the nucleus.

In view of all of these findings, we conclude that the age-related activation of IGF-1R signaling has a more prominent effect on the down regulation of FOXO3a and MnSOD than any other signaling pathway. Transcriptional regulation of MnSOD and catalase makes FOXO3a important in ROS detoxification. MnSOD has been implicated as a key regulator of oxidative stress in scavenging of superoxide in the vessel wall (Li et al, 1995). Aortic superoxide levels were higher in old MnSOD-deficient mice ($MnSOD^{+/-}$) than their age-matched wild-type mice and young counterparts. Furthermore, activation FOXO inhibited VSMC proliferation and neointimal hyperplasia after angioplasty through induction of p27 (Abid et al, 2005).

Finally, IGF-1R signaling potently induced the AP-1 transcription factor by activating ERK. The activated ERK translocated into the nucleus to phosphorylate, and thereby potentiate the transcriptional activity of ternary complex factors (TCFs) to bind to *fos* promoters or directly phosphorylate the Fos proteins (Shaulian and Karin, 2002). The AP-1 transcription factor regulates a wide range of cellular processes, including cell proliferation, death, survival and differentiation. Therefore, age-related activation of IGF-1R signaling poses as a risk for the development of a variety of cardiovascular diseases, including atherosclerosis; while suppression of IGF-1R with its inhibitors may be therapeutically beneficial in enhancing vascular defense to pathogenic stimuli. Future work should confirm the relationships between IGF-1R signaling and atherogenesis in an *in vivo* model of aging and disease.

Acknowledgments

The authors thank Brooke Mossman for scientific advice and Ellen Dimick for assistance in the preparation of the manuscript.

The work was supported by grants from the National Institutes of Health (NIA AG00947 and AG21106).

Literature Cited

Abid M, Yano K, Guo S, Patel VI, Shrikhande G, Spokes KC, Ferran C, Aird WC. Forkhead Transcription Factors Inhibit Vascular Smooth Muscle Cell Proliferation and Neointimal Hyperplasia. J.Biol.Chem. 2005; 280:29864–29873. [PubMed: 15961397]

Arnqvist HJ, Bornfeldt KE, Chen Y, Lindstrom T. The insulin-like growth factor system in vascular smooth muscle: interaction with insulin and growth factors. Metabolism. 1995; 44:58–66. [PubMed: 7476313]

Azar ZM, Mehdi MZ, Srivastava AK. Insulin-like growth factor type-1 receptor transactivation in vasoactive peptide and oxidant-induced signaling pathways in vascular smooth muscle cells. Can.J.Physiol Pharmacol. 2007; 85:105–111. [PubMed: 17487250]

Blough E, Rice K, Desai D, Wehner P, Wright G. Aging alters mechanical and contractile properties of the Fisher 344/Nnia X Norway/Binia rat aorta. Biogerontology. 2007; 8:303–313. [PubMed: 17164981]

Carter ME, Brunet A. FOXO transcription factors. Current Biology. 2007; 17:R113–R114. [PubMed: 17307039]

Delafontaine P, Meng XP, Ku L, Du J. Regulation of vascular smooth muscle cell insulin-like growth factor I receptors by phosphorothioate oligonucleotides. Effects on cell growth and evidence that sense targeting at the ATG site increases receptor expression. J.Biol.Chem. 1995; 270:14383–14388. [PubMed: 7782298]

Delafontaine P, Song YH, Li Y. Expression, regulation, and function of IGF-1, IGF-1R, and IGF-1 binding proteins in blood vessels. Arterioscler Thromb Vasc Biol. 2004; 24:435–444. [PubMed: 14604834]

Dijkers PF, Medema RH, Pals C, Banerji L, Thomas NS, Lam EWF, Burgering BMT, Raaijmakers JAM, Lammers JW, Koenderman L, Coffer PJ. Forkhead Transcription Factor FKHR-L1 Modulates Cytokine-Dependent Transcriptional Regulation of p27KIP1. Mol.Cell.Biol. 2000; 20:9138–9148. [PubMed: 11094066]

Dzau VJ, Braun-Dullaeus RC, Sedding DG. Vascular proliferation and atherosclerosis: new perspectives and therapeutic strategies. Nat Med. 2002; 8:1249–1256. [PubMed: 12411952]

Erol A. JNK/FOXO may be key mechanistic pathway for the hormetic anti-aging. Medical Hypotheses. 2007; 68:923–924. [PubMed: 17064850]

Fried LP. Epidemiology of Aging. Epidemiol Rev. 2000; 22:95–106. [PubMed: 10939013]

Greer EL, Brunet A. FOXO transcription factors at the interface between longevity and tumor suppression. Oncogene. 2005; 24:7410–7425. [PubMed: 16288288]

Hariri RJ, Hajjar DP, Coletti D, Alonso DR, Weksler ME, Rabellino E. Aging and arteriosclerosis. Cell cycle kinetics of young and old arterial smooth muscle cells. Am J Pathol. 1988; 131:132–136. [PubMed: 3354639]

Holzenberger M, Dupont J, Ducos B, Leneuve P, Geloen A, Even PC, Cervera P, Le Bouc Y. IGF-1 receptor regulates lifespan and resistance to oxidative stress in mice. Nature. 2003; 421:182–187. [PubMed: 12483226]

Honda Y, Honda S. The daf-2 gene network for longevity regulates oxidative stress resistance and Mn-superoxide dismutase gene expression in Caenorhabditis elegans. FASEB J. 1999; 13:1385–1393. [PubMed: 10428762]

Johansson GS, Arnqvist HJ. Insulin and IGF-I action on insulin receptors, IGF-I receptors, and hybrid insulin/IGF-I receptors in vascular smooth muscle cells. Am J Physiol Endocrinol Metab. 2006; 291:E1124–E1130. [PubMed: 16803852]

Kops GJPL, Dansen TB, Polderman PE, Saarloos I, Wirtz KWA, Coffer PJ, Huang TT, Bos JL, Medema RH, Burgering BMT. Forkhead transcription factor FOXO3a protects quiescent cells from oxidative stress. Nature. 2002; 419:316–321. [PubMed: 12239572]

Lee HY, Chung JW, Youn SW, Kim JY, Park KW, Koo BK, Oh BH, Park YB, Chaqour B, Walsh K, Kim HS. The Forkhead Transcription Factor FOXO3a Is a Negative Regulator of Angiogenic Immediate Early Gene CYR61, Leading to Inhibition of Vascular Smooth Muscle Cell Proliferation and Neointimal Hyperplasia. Circ Res. 2007; 01

Li C, Xu Q. Mechanical stress-initiated signal transduction in vascular smooth muscle cells in vitro and in vivo. Cellular Signalling. 2007; 19:881–891. [PubMed: 17289345]

Li M, Liu RM, Timblin CR, Meyer SG, Mossman BT, Fukagawa NK. Age affects ERK1/2 and NRF2 signaling in the regulation of GCLC expression. J Cell Physiol. 2006a; 206:518–525. [PubMed: 16155909]

Li M, Mossman BT, Kolpa E, Timblin CR, Shukla A, Taatjes DJ, Fukagawa NK. Age-related differences in MAP kinase activity in VSMC in response to glucose or TNF-alpha. J.Cell Physiol. 2003; 197:418–425. [PubMed: 14566971]

Li M, Chiu JF, Mossman BT, Fukagawa NK. Down-regulation of Manganese-Superoxide Dismutase through Phosphorylation of FOXO3a by Akt in Explanted Vascular Smooth Muscle Cells from Old Rats. J.Biol.Chem. 2006b; 281:40429–40439. [PubMed: 17079231]

Li Y, Huang TT, Carlson EJ, Melov S, Ursell PC, Olson JL, Noble LJ, Yoshimura MP, Berger C, Chan PH, Wallace DC, Epstein CJ. Dilated cardiomyopathy and neonatal lethality in mutant mice lacking manganese superoxide dismutase. Nat Genet. 1995; 11:376–381. [PubMed: 7493016]

Liang J, Zubovitz J, Petrocelli T, Kotchetkov R, Connor MK, Han K, Lee JH, Ciarallo S, Catzavelos C, Beniston R, Franssen E, Slingerland JM. PKB/Akt phosphorylates p27, impairs nuclear import of p27 and opposes p27-mediated G1 arrest. Nat Med. 2002; 8:1153–1160. [PubMed: 12244302]

Lim HJ, Park HY, Ko YG, Lee SH, Cho SY, Lee EJ, Jameson JL, Jang Y. Dominant negative insulin-like growth factor-1 receptor inhibits neointimal formation through suppression of vascular smooth muscle cell migration and proliferation, and induction of apoptosis. Biochemical and Biophysical Research Communications. 2004; 325:1106–1114. [PubMed: 15541402]

Longo VD, Finch CE. Evolutionary medicine: from dwarf model systems to healthy centenarians? Science. 2003; 299:1342–1346. [PubMed: 12610293]

Maier B, Gluba W, Bernier B, Turner T, Mohammad K, Guise T, Sutherland A, Thorner M, Scrable H. Modulation of mammalian life span by the short isoform of p53. Genes Dev. 2004; 18:306–319. [PubMed: 14871929]

Manfroid I, Van de Weerdt C, Baudhuin A, Martial JA, Muller M. EGF stimulates Pit-1 independent transcription of the human prolactin pituitary promoter in human breast cancer SK-BR-3 cells through its proximal AP-1 response element. Molecular and Cellular Endocrinology. 2005; 229:127–139. [PubMed: 15607537]

Menu E, Kooijman R, Van Valckenborgh E, Asosingh K, Bakkus M, Van Camp B, Vanderkerken K. Specific roles for the PI3K and the MEK-ERK pathway in IGF-1-stimulated chemotaxis, VEGF secretion and proliferation of multiple myeloma cells: study in the 5T33MM model. Br.J.Cancer. 2004; 90:1076–1083. [PubMed: 14997210]

Miller SJ, Watson WC, Kerr KA, Labarrere CA, Chen NX, Deeg MA, Unthank JL. Development of progressive aortic vasculopathy in a rat model of aging. Am J Physiol Heart Circ Physiol. 2007; 293:H2634–H2643. [PubMed: 17873024]

Najjar SS, Scuteri A, Lakatta EG. Arterial Aging: Is It an Immutable Cardiovascular Risk Factor? Hypertension. 2005; 46:454–462. [PubMed: 16103272]

Nemoto S, Finkel T. Redox Regulation of Forkhead Proteins Through a p66shc-Dependent Signaling Pathway. Science. 2002; 295:2450–2452. [PubMed: 11884717]

Nichols TC, Laney T.d. Zheng B, Bellinger DA, Nickols GA, Engleman W, Clemmons DR. Reduction in Atherosclerotic Lesion Size in Pigs by {alpha}V{beta}3 Inhibitors Is Associated With Inhibition of Insulin-Like Growth Factor-I-Mediated Signaling. Circ Res. 1999; 85:1040–1045. [PubMed: 10571535]

Nosaka Y, Arai A, Kanda E, Akasaki T, Sumimoto H, Miyasaka N, Miura O. Rac Is Activated by Tumor Necrosis Factor [alpha] and Is Involved in Activation of Erk. Biochemical and Biophysical Research Communications. 2001; 285:675–679. [PubMed: 11453646]

Parrizas M, Gazit A, Levitzki A, Wertheimer E, LeRoith D. Specific Inhibition of Insulin-Like Growth Factor-1 and Insulin Receptor Tyrosine Kinase Activity and Biological Function by Tyrphostins. Endocrinology. 1997; 138:1427–1433. [PubMed: 9075698]

Pennathur S, Heinecke JW. Mechanisms for oxidative stress in diabetic cardiovascular disease. Antioxid.Redox.Signal. 2007; 9:955–969. [PubMed: 17508917]

Rice KM, Kinnard RS, Harris R, Wright GL, Blough ER. Effects of aging on pressure-induced MAPK activation in the rat aorta. Pflugers Arch. 2005a; 450:192–199. [PubMed: 15877234]

Rice KM, Kinnard RS, Wright GL, Blough ER. Aging alters vascular mechanotransduction: Pressure-induced regulation of p70S6k in the rat aorta. Mechanisms of Ageing and Development. 2005b; 126:1213–1222. [PubMed: 16087221]

Russell JW, Golovoy DAVI, Vincent AM, Mahendru PIA, Olzman JA, Mentzer ALIC, Feldman EL. High glucose-induced oxidative stress and mitochondrial dysfunction in neurons. FASEB J. 2002; 16:1738–1748. [PubMed: 12409316]

Scheidegger KJ, Cenni B, Picard D, Delafontaine P. Estradiol decreases IGF-1 and IGF-1 receptor expression in rat aortic smooth muscle cells. Mechanisms for its atheroprotective effects. J.Biol.Chem. 2000a; 275:38921–38928. [PubMed: 10982795]

Scheidegger KJ, James RW, Delafontaine P. Differential effects of low density lipoproteins on insulin-like growth factor-1 (IGF-1) and IGF-1 receptor expression in vascular smooth muscle cells. J Biol Chem. 2000b; 275:26864–26869. [PubMed: 10862615]

Schwartz SM. Smooth Muscle Migration in Atherosclerosis and Restenosis. J.Clin.Invest. 1997; 99:2814–2816. [PubMed: 9185501]

Shaulian E, Karin M. AP-1 as a regulator of cell life and death. Nature Cell Biology. 2002; 4:E131.

Shin I, Yakes FM, Rojo F, Shin NY, Bakin AV, Baselga J, Arteaga CL. PKB/Akt mediates cell-cycle progression by phosphorylation of p27Kip1 at threonine 157 and modulation of its cellular localization. Nat Med. 2002; 8:1145–1152. [PubMed: 12244301]

Spinetti G, Wang M, Monticone R, Zhang J, Zhao D, Lakatta EG. Rat Aortic MCP-1 and Its Receptor CCR2 Increase With Age and Alter Vascular Smooth Muscle Cell Function. Arterioscler Thromb Vasc Biol. 2004; 24:1397–1402. [PubMed: 15178559]

Sprott RL, Ramirez I. Current Inbred and Hybrid Rat and Mouse Models for Gereontological Research. ILAR.J. 1997; 38:104–109. [PubMed: 11528051]

Utsugi M, Dobashi K, Ishizuka T, Masubuchi K, Shimizu Y, Nakazawa T, Mori M. C-Jun-NH2-Terminal Kinase Mediates Expression of Connective Tissue Growth Factor Induced by Transforming Growth Factor-{beta}1 in Human Lung Fibroblasts. Am.J.Respir.Cell Mol.Biol. 2003; 28:754–761. [PubMed: 12760970]

Vazquez-Padron RI, Lasko D, Li S, Louis L, Pestana IA, Pang M, Liotta C, Fornoni A, Aitouche A, Pham SM. Aging exacerbates neointimal formation, and increases proliferation and reduces susceptibility to apoptosis of vascular smooth muscle cells in mice. J.Vasc.Surg. 2004; 40:1199–1207. [PubMed: 15622375]

Wang MC, Bohmann D, Jasper H. JNK Extends Life Span and Limits Growth by Antagonizing Cellular and Organism-Wide Responses to Insulin Signaling. Cell. 2005; 121:115–125. [PubMed: 15820683]

Werner H, Maor S. The insulin-like growth factor-I receptor gene: a downstream target for oncogene and tumor suppressor action. Trends in Endocrinology & Metabolism. 2006; 17:236–242. [PubMed: 16815029]

Zhu B, Zhao G, Witte DP, Hui DY, Fagin JA. Targeted Overexpression of IGF-I in Smooth Muscle Cells of Transgenic Mice Enhances Neointimal Formation through Increased Proliferation and Cell Migration after Intraarterial Injury. Endocrinology. 2001; 142:3598–3606. [PubMed: 11459808]

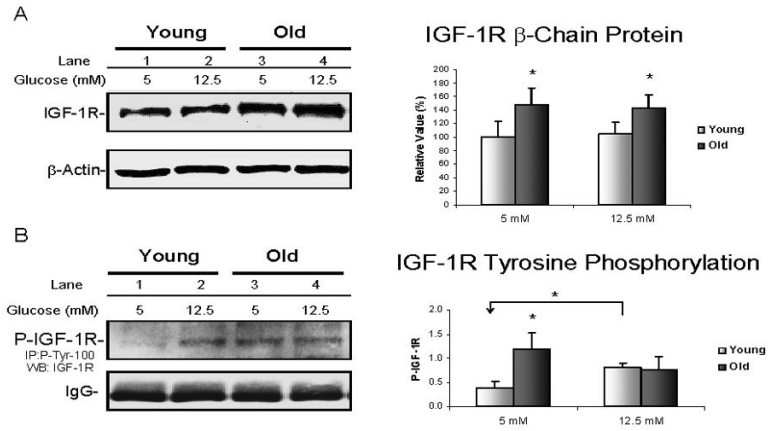

Fig. 1. Assessment of IGF-1R activity

VSMC from 4 pairs of young (6 mo) and old (24 mo) rats were grown in DMEM containing 5 mM (control), 12.5 mM (high) glucose for 3 days. Cytoplasmic proteins were isolated after cell lysis. **A**. Example of a Western blot using anti-IGF-1R β chain antibody is shown on left; β-actin antibody was used as a loading control. On the right, changes of IGF-1R β-chain protein level for young (☐) and old (■) rats are presented as a percentage of young control values (mean ± SE, n=4 per group). The individual *p* value is described in the text, and * denotes $p \leq 0.05$ for comparisons between young and old. **B**. On the left, a representative blot that was IP by P-Tyr-100 and immunoblotted with IGF-1R antibodies shows IGF-1R autophosphorylation status. The additional panel of IgG was included below to show that equal amounts of P-Tyr-100 antibody were loaded in IP. On the right, a summary of autophosphorylated IGF-1R β chain for young (☐) and old (■) rats expressed as mean ± SE (n=4 per group). The *p* values were as described in the text, and * denotes $p \leq 0.05$ for comparisons between young and old or for comparison between the indicated pairs.

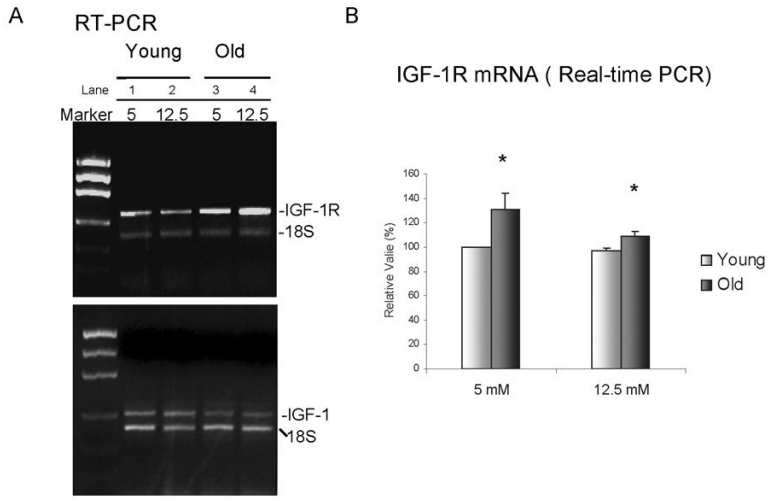

Fig. 2. Quantification of IGF-1R gene expression

VSMC from 4 pairs of young (6 mo) and old (24 mo) rats were grown in DMEM containing 5 mM (control) or 12.5 mM glucose for 3 days. **A.** Two representative RT-PCR gels show the 516 bp IGF-1R bands with 315 bp 18S-RNA control on the top; and the 424 bp of IGF-1 bands with the same 18S-RNA bands on the bottom. **B.** Expression of IGF-1R (n=4 per group) were quantified by custom-designed TaqMan®Gene Expression Assay on ABI Prism 7700. The individual p value is described in the text, and * indicates $p \leq 0.05$ for comparisons between young (□) and old (■).

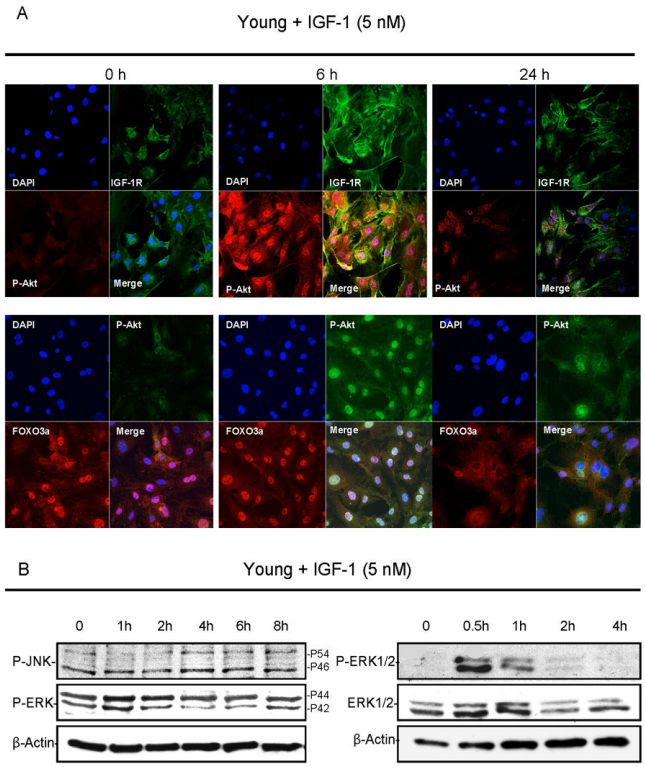

Fig. 3. Effect of IGF-1 on IGF-1R signaling

VSMC from young rats were grown in complete DMEM medium overnight and then changed to reduced medium with 5 nM IGF-1 for 0.5, 1, 2, 4, 6, 8 or 24 h. **A.** Images depicting the shuttling of P-Akt and P-FOXO3a between the nucleus and cytosol at the indicated times were captured using a confocal laser scanning microscope and shown in two panels: on the top, slides stained with anti-IGF-1R in green, anti-P-Akt in red; on the bottom, slides stained with anti-P-Akt in red and FOXO3a in green; both with DAPI-stained nuclei in purple. Each image includes three splits of single channel and one merged of three channels. **B.** On the left, an example of a Western blot shows cytoplasmic P-JNK vs. P-ERK after 0, 1, 2, 4, 6, 8 h of IGF-1 exposure with corresponding β-actin as a loading control. On the right, an example of a Western blot shows P-ERK1/2 vs. total ERK1/2 after 0, 0.5, 1, 2, and 3 h of IGF-1 exposure with the corresponding β-actin blot as a loading control.

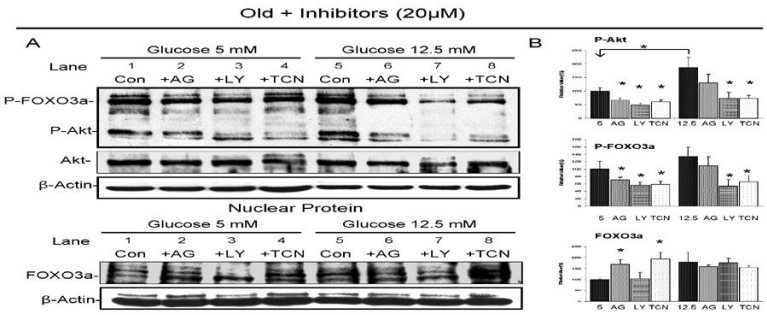

Fig. 4. Effect of kinase inhibitors on Akt/FOXO pathway

VSMC from three old rats were sub-cultured overnight and on the second day, cells were pre-treated with 20 μM of AG1024, LY294002, or TCN for 30 min and then grown for 3 days in medium containing 5 mM or 12.5 mM glucose with 20 μM of each inhibitor, respectively. **A.** Upper panel shows a blot of P-Akt together with P-FOXO3a and a blot of Akt in total protein; lower panel shows total FOXO3a in nuclear extracts. Each includes the same blot of β-actin as loading control. **B.** Changes of P-FOXO3a, P-Akt levels and FOXO3a in AG1024-, LY294002-, and TCN-treated cells are summarized as a percentage of 5 mM glucose control (mean ± SE). The individual of p values are described in the text and * indicates $p \leq 0.05$ for comparisons between the cells treated with inhibitors and corresponding controls, or alternatively, as indicated between the cells grown in 5 mM and 12.5 mM glucose medium.

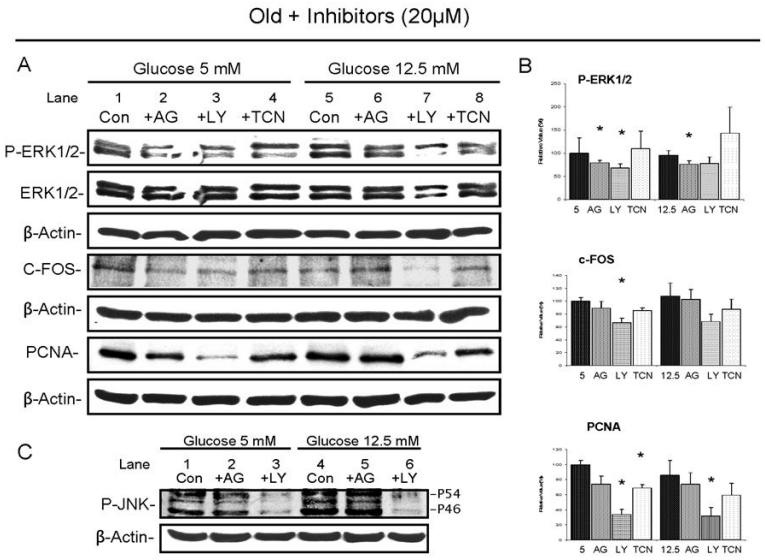

Fig. 5. Effect of kinase inhibitors on MAPK/AP-1 pathway

VSMC from three old rats were sub-cultured overnight and on the second day, cells were pre-treated with 20μM of AG1024, LY294002, or TCN for 30 min and then grown for 3 days in medium containing 5 mM or 12.5 mM glucose with 20 μM of each inhibitor, respectively. **A.** Examples of Western blots showing P-ERK1/2, ERK1/2 and PCNA in total proteins, c-Fos in nuclear proteins. Each includes the same blot of β-actin as loading control. **B.** Changes of P-ERK1/2, c-Fos and PCNA in AG1024-, LY294002-, and TCN-treated cells summarized as a percentage of 5 mM glucose control (mean ± SE). The individual of p values are described in the text and the * indicates $p \leq 0.05$ for comparisons between cells treated with inhibitors and corresponding controls. **C.** An example of Western blots comparing the effect of AG1024 with LY294002 on P-JNK changes in total proteins.

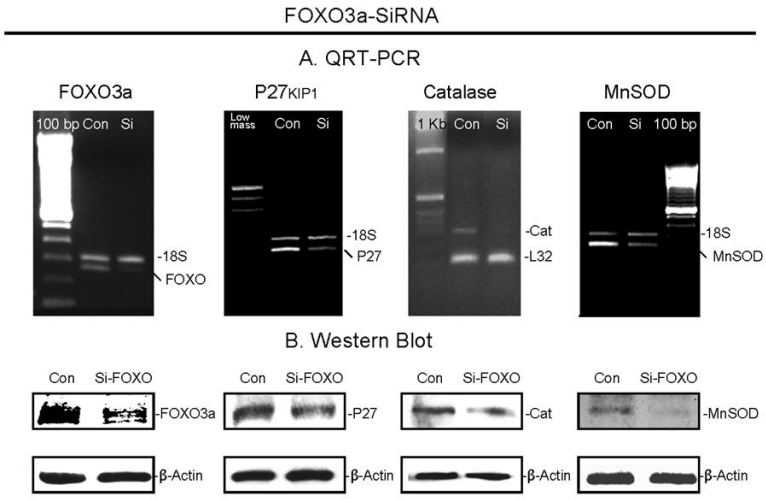

Fig.6. Effect of si-FOXO3a on expression of p27, catalase and MnSOD

VSMC were transfected with 100 nM si-FOXO3a or control for 48 h followed by RNA and protein extraction. **A.** Examples of semi-quantitative RT-PCR showing si-FOXO3a-treated FOXO3a, p27, catalase and MnSOD bands vs. control, respectively. 18S RNA was simultaneously amplified as the loading control. **B.** Examples of Western blot showing the protein changes between si-FOXO3a-transfected and control VSMC.

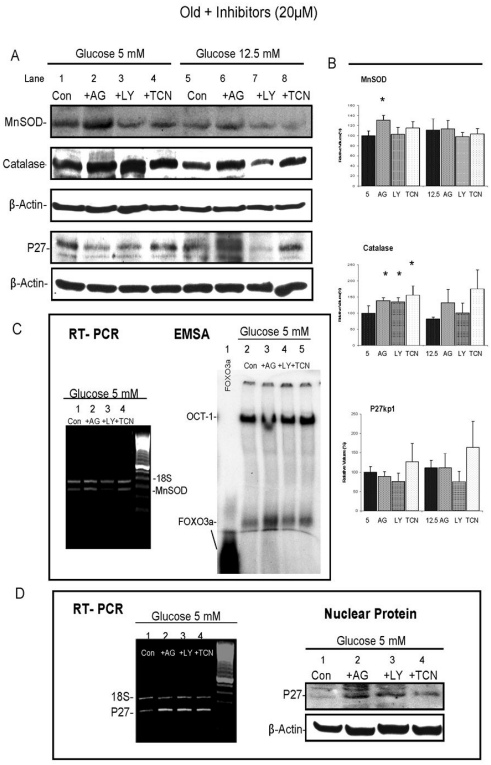

Fig. 7. Effect of kinase inhibitors on MnSOD, catalase and p27

VSMC from three old rats were sub-cultured overnight and on the second day, cells were pre-treated with 20μM of AG1024, LY294002, or TCN for 30 min and then grown for 3 days in medium containing 5 mM or 12.5 mM glucose with 20 μM of each inhibitor, respectively. **A.** Examples of Western blots showing MnSOD and catalase in cytoplasmic protein and p27 in total protein. Each includes the same blot with β-actin as a loading control. **B.** Changes of MnSOD, catalase and p27 in AG1024-, LY294002-, and TCN-treated cells summarized as a percentage of 5 mM glucose control (mean ± SE, n=3). *p* values are for comparisons between the cells treated with inhibitors in 5 mM glucose or 12.5 mM glucose medium vs. their corresponding controls, and * indicates $p \leq 0.05$. **C.** On the left is an example of quantitative-RT-PCR showing dual amplification of MnSOD and 18S RNA bands from a set of VSMC grown in 5 mM glucose medium with or without inhibitors. On the right, an EMSA result shows the corresponding activity of FOXO3a binding to MnSOD detected by radioactively-labeled MnSOD-DBE probe. In addition, an OCT-1 consensus was used as an internal loading control, and binding between the 100-residue of the FOXO3a peptide and MnSOD-DBE probe is included in lane 1. **D.** On the left, an example of quantitative-RT-PCR showing dual amplification of p27 and 18S RNA bands from a set of VSMC grown in 5 mM glucose medium with or without inhibitors. On the right, an example of a Western blots shows changes of p27 protein in the nucleus of VSMC grown in 5 mM glucose with inhibitors.